Postharvest Biology and Technology 86 (2013) 424–430

Contents lists available at ScienceDirect

Postharvest Biology and Technology

journal homepage: www.elsevier.com/locate/postharvbio

Early decay detection in citrus fruit using laser-light backscattering imaging

D. Lorente[a], M. Zude[b], C. Regen[b], L. Palou[c], J. Gómez-Sanchis[d], J. Blasco[a,*]

[a] Centro de Agroingenieria, Instituto Valenciano de Investigaciones Agrarias (IVIA), Cra. Moncada-Náquera km 5, Moncada, 46113 Valencia, Spain
[b] Leibniz-Institute for Agricultural Engineering Potsdam-Bornim (ATB), Max-Eyth-Allee 100, 14469 Potsdam-Bornim, Germany
[c] Centro de Tecnología Poscosecha (CTP), Instituto Valenciano de Investigaciones Agrarias (IVIA), Cra. Moncada-Náquera km 5, Moncada, 46113 Valencia, Spain
[d] Intelligent Data Analysis Laboratory (IDAL), Electronic Engineering Department, Universitat de València, Avda. Universitat s/n, Burjassot, 46100 Valencia, Spain

ARTICLE INFO

Article history:
Received 12 April 2013
Accepted 8 July 2013

Keywords:
Fruit inspection
Citrus fruit
Decay
Laser-light backscattering imaging
LDA classifier
Gaussian–Lorentzian cross product function

ABSTRACT

Early detection of fungal infections in citrus fruit still remains one of the major problems in postharvest technology. The potential of laser-light backscattering imaging was evaluated for detecting decay in citrus fruit after infection with the pathogen *Penicillium digitatum*, before the appearance of fruiting structures (green mould). Backscattering images of oranges cv. Navelate with and without decay were obtained using diode lasers emitting at five different wavelengths in the visible and near infrared range for addressing the absorption of fruit carotenoids, chlorophylls and water/carbohydrates. The apparent region of backscattered photons captured by a camera had radial symmetry with respect to the incident point of the light, being reduced to a one-dimensional profile after radial averaging. The Gaussian–Lorentzian cross product (GL) distribution function with five independent parameters described radial profiles accurately with average R^2 values higher or equal to 0.998, pointing to differences in the parameters at the five wavelengths between sound and decaying oranges. The GL parameters at each wavelength were used as input vectors for classifying samples into sound and decaying oranges using a supervised classifier based on linear discriminant analysis. Ranking and combination of the laser wavelengths in terms of their contribution to the detection of decay resulted in the minimum detection average success rate of 80.4%, which was obtained using laser light at 532 nm that addresses differences in scattering properties of the infected tissue and carotenoid contents. However, the best results were achieved using the five laser wavelengths, increasing the classifier average success rate up to 96.1%. The results highlight the potential of laser-light backscattering imaging for advanced citrus grading.

1. Introduction

Decay caused by *Penicillium* spp. is among the main problems affecting postharvest and marketing processes of citrus fruit (Palou et al., 2011). Early detection of fungal infections still remains one of the major issues in packinghouses because a small number of decayed fruit can cause the infection of a whole consignment during storage and distribution. Currently, the detection of decayed fruit in packing lines is carried out visually by trained workers inspecting each fruit individually as it passes under ultraviolet (UV) light along a conveyor belt. However, this procedure has a high risk of human error and is potentially harmful for operators (Lopes et al., 2010). Machine vision systems potentially provide a means to detect decayed fruit automatically, thus preventing the drawbacks related to human inspection.

Although the use of technology based on colour cameras has spread rapidly for detecting skin damage of fruit and vegetables (cf. Zude, 2009; Cubero et al., 2011), its application to the external inspection of citrus fruit is only currently under research. For example, Kim et al. (2009) detected peel diseases in grapefruit using colour texture features based on HSI (Hue, Saturation, Intensity) and the colour co-occurrence method. Nevertheless, some defects, such as decay at very early stages, are virtually identical to the sound skin, thus very difficult to detect by the human eye, and consequently, by standard artificial vision systems, which are limited to the visible region of the electromagnetic spectrum (Blasco et al., 2009).

Various machine vision technologies have been incorporated for automatically detecting decay in citrus fruit imitating the fluorescence technique used in the industry by humans. Kurita et al. (2009) developed an inspection system based on two lighting systems

* Corresponding author. Tel.: +34 963424000; fax: +34 963424001.
E-mail address: blasco_josiva@gva.es (J. Blasco).

0925-5214/$ – see front matter © 2013 Elsevier B.V. All rights reserved.
http://dx.doi.org/10.1016/j.postharvbio.2013.07.021

Fig. 1. RGB images of a sound orange used for a control (*left*) and an orange showing early decay symptoms caused by *P. digitatum* (*right*).

(visible and UV) that should be powered alternatively using a stroboscopic mode since the fluorescence effect produced by UV light would be undetectable with a simultaneous use of both systems due to the high intensity of white light. However, the use of UV light has some limitations because not all decay lesions, and not all the citrus cultivars, present the same level of sensitivity to the fluorescence phenomena, and on the contrary, other defects like chilling injury can result in some fluorescence (Slaughter et al., 2008), thus reducing the performance of these systems. In this sense, the recent introduction of hyperspectral sensors for food inspection is a successful alternative to detect non-visible damages on fruit (Lorente et al., 2012b). In the particular case of citrus fruit, different research has been conducted to detect decay lesions. For instance, Gómez-Sanchis et al. (2012, 2013) and Lorente et al. (2012a, 2013) studied the feasibility of a hyperspectral vision system based on liquid crystal tuneable filters (LCTF; 460–1020 nm) for detecting decay in citrus fruit in early stages of infection using halogen lighting instead of the traditional inspection using UV lighting.

Recently, light backscattering imaging (LBI) has been studied as an alternative machine vision technique for assessing fruit quality. When a light beam interacts with a fruit, reflectance, absorption and transmittance occur (Birth, 1976). Particularly, light reflectance (scattering) appears with two different geometries: Fresnel reflectance, which happens when photons are reflected on the surface of the sample; and diffuse reflectance (Meinke and Friebel, 2009). In the latter case, light enters the sample and interacts with the internal components of the fruit, and then it is scattered backward to the exterior tissue surface, thus carrying information related to the morphology and structures of the tissue additional to the absorption properties (Lu, 2004). In recent years, much work has focused on using LBI systems to assess quality of apples and other fresh fruit; however, no research has been reported to detect decay in citrus fruit using this technique. For example, Lu (2004) analyzed backscattering images from apples at multiple wavelengths in the visible and the near-infrared (NIR) region for predicting firmness and soluble solids content. In another study, the variation of moisture content of banana slices subjected to different drying conditions was evaluated by taking backscattering images at 670 nm (Romano et al., 2008). From experiments on bruised apples, Lu et al. (2010) suggested that the scattering analysis would provide good results.

Decay process in citrus fruit implies changes in enzymatic activity, resulting in an enhanced water-soluble pectin fraction, and consequently, weakening of the cell wall (Barmore and Brown, 1979). The subsequent water soaking of the tissue is an early visible symptom of infection in citrus (Barmore and Brown, 1981). Hence, since later changes in the pigment contents, and therefore in the optical properties of fruit tissue, can be expected, the LBI technique could be a promising tool for detecting decay in citrus fruit. The main objective of this research work was to evaluate the potential of laser-light backscattering imaging as a tool for the automatic detection of green mould caused by *P. digitatum* on citrus fruit. For this purpose, diode lasers emitting in the visible and NIR range were used to obtain backscattering images of citrus fruit aiming for the classification of fruit into two classes (sound and decaying oranges). The ultimate aim of this work was to evaluate and compare laser wavelengths in terms of their contribution to the detection of decay.

2. Materials and methods

2.1. Fruit and fungal inoculation

The experiments were carried out using sweet oranges (*Citrus sinensis* L. Osbeck) cv. Navelate collected during the 2012 harvest season from the field collection of the Citrus Germplasm Bank at the IVIA (Spain) (Navarro et al., 2002). A total of 100 fruit were used for the experiments: 50 oranges were superficially injured on the rind and inoculated with spores of *P. digitatum* and the other 50 were injured in the same way but treated with sterilized water for control purposes. *P. digitatum* isolate NAV-7, from the fungal culture collection of the IVIA CTP, was cultured on potato dextrose agar (PDA, Sigma–Aldrich Chemical Co., St. Louis, MA, USA) plates at 25 °C. Conidia from 7 to 14 day old cultures were taken from the agar surface with a sterile glass rod and transferred to a sterile aqueous solution of 0.05% Tween® 80 (Panreac, S.A.U., Spain). The conidial suspension was filtered through two layers of cheesecloth to separate hyphal fragments and adjusted to a concentration of 10^6 spores/mL using a haemocytometer. For inoculation, 20 μL of the conidial suspension was placed on the equator of each fruit by immersing the tip of a stainless steel rod, 1 mm wide and 2 mm in length, in the suspension and inserting it in the fruit rind. A concentration of 10^6 spores/mL of *P. digitatum* is the most appropriate to effectively infect citrus fruit in laboratory conditions (Palou et al., 2001). The fruit were stored for four days in a controlled environment at 20 °C and 65% RH. After this period, all the inoculated fruit presented lesions due to decay of an average diameter of 30 mm. Fig. 1 shows the images of a sound control orange and an infected orange.

2.2. Imaging system

In this work, a laser light backscattering imaging system was employed. This system mainly consisted of a CCD (charge-coupled device) based camera (JAI CV-A50 IR) with a zoom lens (F2.5 and

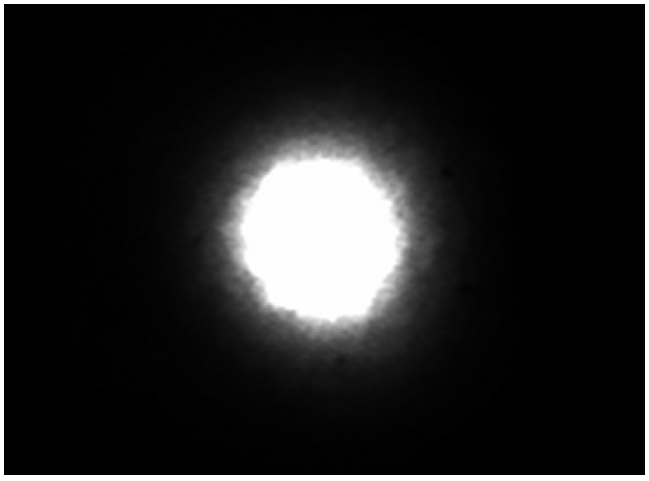

Fig. 2. Example of a raw backscattering image.

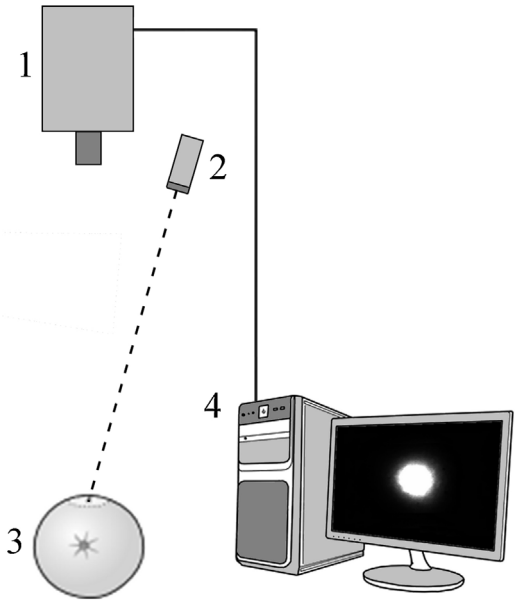

Fig. 3. Scheme of the laser light backscattering system. 1: CCD camera with lens; 2: laser source; 3: fruit sample; and 4: computer.

focal lengths of 18–108 mm), five solid-state laser diode modules emitting at different wavelengths (532, 660, 785, 830 and 1060 nm) used alternately as light sources and a computer for controlling the camera. After penetrating into the fruit tissue, the fraction of the light backscattered to the fruit surface was recorded by the camera and transferred to the computer. A typical raw backscattering image is shown in Fig. 2.

The imaging system was set up in a dark room in order to prevent the influence of ambient light. It was configured to acquire 720 × 576 pixel images with a resolution of 0.073 mm/pixel. Parameters of laser sources are shown in Table 1. The incident angle of the light beam was set to 7° with respect to the vertical axis for all the laser sources and the distance from the laser sources to the fruit sample was chosen according to the focus of each laser (Qing et al., 2007). This setting allowed for the assumption that the light beam was almost perpendicular to the fruit surfaces, thus obtaining images symmetric with respect to the incident point (Mollazade et al., 2012). The arrangement of the image acquisition system is pictured in Fig. 3. The backscattering images were acquired by placing the fruit manually in the imaging system presenting the damage to the camera. A total of five images were acquired for each of the 100 orange samples at the five laser wavelengths which gave a total number of 500 backscattering images.

2.3. Function for describing backscattering profiles

Backscattering images had radial symmetry with respect to the light incident point and their intensity decreases with increasing distance from the incident point (Fig. 2). The images were reduced to one-dimensional profiles after radial averaging (Lu, 2004). For this purpose, the centre of beam incident point was identified for each backscattering image using the weighted centre of gravity method (Weeks, 1996), which considers that the centre is a point in which the maximum light intensity occurs. The radial intensity of the backscattering profiles was then calculated by obtaining the average value of all pixels within each circular ring with one pixel size (0.073 mm).

Backscattering profiles thus obtained could be used directly as a feature vector to predict the presence of damage on the skin of the fruit by a multivariate calibration model. In order to get more robust and fast predictions, data reduction was targeted. One method for this is to find the parameters of symmetric distribution functions describing the backscattering profiles.

Moreover, it is advisable to perform some pre-processing on the profiles to fit the backscattering profiles more accurately, such as removing the data points within and adjacent to the light incident area since these points are saturated, or shifting the profiles towards the profile centre by a distance equal to the number of removed data points in the saturation area (Peng and Lu, 2005). In this work, all the data points with a greyscale level (0–255) higher than 253 were removed.

Subsequently to pretests using various distribution functions (data not shown), the Gaussian–Lorentzian cross product (GL) function was applied. This distribution function is a Voigt approximation that combines a Gaussian and a Lorentzian in a multiplicative form. GL is commonly used in spectroscopy; also for describing laser profiles (Penache et al., 2002; Limandri et al., 2008; Stace et al., 2012). The GL function is mathematically expressed by Eq. (1):

$$I(x) = a + \frac{b}{[1 + e((x-c)/d)^2]\exp[((1-e)/2)((x-c)/d)^2]} \quad (1)$$

where I is the light intensity of each circular band after radial averaging; x is the scattering distance expressed as number of data points (pixels); a is the asymptotic value of light intensity when x approaches infinity; b is the peak value of estimated light intensity at the centre; c is the centre parameter; d is the full scattering width that produces the half maximum peak value; e is related to the shape. The shape parameter e varies from 0 to 1; a value of 0 results in the pure Gaussian function, whereas the pure Lorentzian occurs with a value of 1. Fig. 4 shows a backscattering profile described by this GL distribution function with five parameters.

The GL function was used to fit the backscattering profiles at the five laser wavelengths for each fruit sample. A programme based on nonlinear least squares regression analysis (Gelman and Hill, 2006)

Table 1
Parameters of laser sources.

Wavelength (nm)	Output (mW)	Beam size (mm)
532	10	2.5 × 2.5
660	2	4.0 × 4.0
785	45	1.0 × 1.0
830	30	1.0 × 1.0
1060	85	1.5 × 5.25

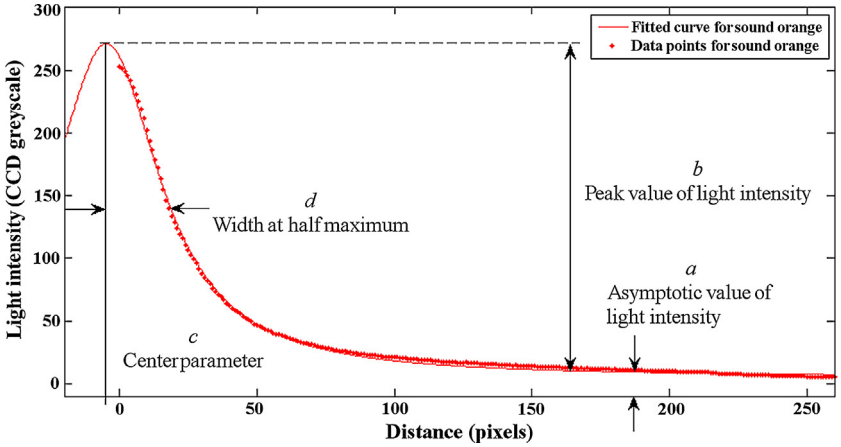

Fig. 4. Gaussian–Lorentzian cross product distribution model for backscattering profiles.

was written using Curve Fitting Toolbox of Matlab 7.9 (Mathworks, Inc.) in order to fit the backscattering profiles to the GL function and to estimate the five GL parameters for each sample at each laser wavelength. The remaining algorithms in this work, such as classification methods, were also implemented using Matlab environment.

2.4. Classifier

Linear discriminant analysis (LDA), also known as Fisher discriminant analysis (Fisher, 1936), is a supervised method of dimensionality reduction and classification used in statistics, pattern recognition and machine learning (Sierra, 2002; Wang et al., 2011). LDA aims to find a linear projection of high-dimensional data onto a lower dimensional space ($c-1$ dimensions in a problem with c classes) where the class separation is maximized. This is achieved by maximizing the ratio of the variance between the classes and variance within the classes (Duda et al., 2001). LDA has no free parameters to be adjusted and the extracted features are potentially interpretable under linearity assumptions. Furthermore, LDA is closely related to principal component analysis (PCA). The main difference between both linear projection techniques is that LDA explicitly attempts to model the difference between the classes of data, while PCA does not take into account any difference in class due to its unsupervised nature. LDA method therefore performs better for classification purposes (Martínez and Kak, 2004).

2.5. Labelled set

In supervised classification, there is a set of n labelled samples, $\{\mathbf{x}_i, t_i\}_{i=1..n}$, where x_i represents the m-dimensional feature vector for the i-th sample with label t_i In this work, the supervised nature of the LDA classifier required the construction of a labelled data set, consisting of $m=25$ features associated to each orange sample, specifically the five GL parameters at each of the five laser wavelengths obtained from fitting the profiles.

In order to build this labelled set, the $n=100$ oranges were assigned to one of the two classes considered in this work: sound oranges and oranges presenting decay. Each sample pattern was therefore composed by 25 features and a class label. The labelled set was divided into a calibration set of 50 samples (50% of the total) and a validation set of 50 samples (50% of the total). The first set was used to build the proposed classification method and the second one to evaluate its performance. In the validation set, the same number of samples as in the calibration set was chosen in order to check the generalization capability of the classifier.

2.6. Development and validation of the classification models

LDA classification method and parameters obtained with GL at five laser wavelengths were used to classify fruit samples. Laser wavelengths were ranked in terms of their contribution to decay detection. In order to rank wavelengths, the LDA classifier was first build and evaluated using the five GL parameters corresponding to each individual wavelength as feature vector. Laser wavelengths were then ranked in ascending order of classification average success rate values. The best single wavelength that had the highest success rate was selected. The next step is to obtain the best two wavelengths. Each of the remaining wavelengths was individually added to the best single wavelength, and the corresponding success rate values were computed for all two-wavelength combinations. The best two wavelengths were chosen when they had the highest success rate among all two-wavelength combinations. This procedure was then repeated for obtaining the best three wavelengths and so on, until all wavelengths were ranked.

The calibration set of labelled data was used to build the classification models and the validation set to evaluate classifier performance. Apart from calculating the classification average success rates to assess the performance of classification, Cohen's kappa statistic values were computed to evaluate the classification bias (Fleiss, 1981). Classification average success rate provided a measure for classification accuracy with a range from 0% to 100%, this parameter being calculated as the number of correctly classified samples divided by the total number of samples. Cohen's kappa statistic gave information about if classifier was biased towards one of the two classes, varying from 0 to 1, with a value of 1 representing a completely unbiased classifier.

3. Results and discussion

3.1. Description of backscattering profiles

For the five laser wavelengths, the GL function described backscattering profiles with average R^2 values higher or equal to 0.998 and average RMSE lower or equal to 2.54 (CCD greyscale) (Table 2). These values were calculated by averaging the coefficients of determination and the RMSEs corresponding to the 100 orange samples at each laser wavelength.

The average GL parameters and the resulting average fitted curves obtained for the backscattering profiles of sound oranges and oranges with decay at the five laser wavelengths are shown in Fig. 5. A significance test (p-value <0.05, one-tailed paired t-test) was applied to the data in order to determine if the differences between average parameters of sound oranges and decaying

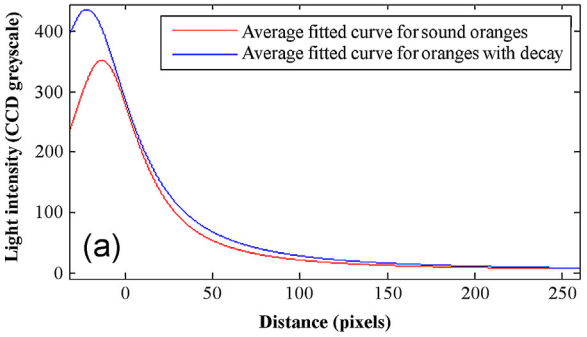

	Sound	Decaying
a (greyscale)*	3.72	2.99
b (greyscale)*	348.80	433.64
c (pixels)*	-13.30	-21.84
d (pixels *	25.97	30.27
e (unitless)	1.000	0.999

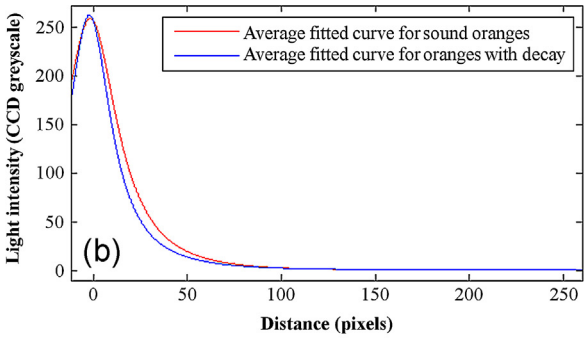

	Sound	Decaying
a (greyscale)*	0.97	0.98
b (greyscale)	257.75	261.57
c (pixels)	-1.65	-2.13
d (pixels)*	16.97	13.67
e (unitless)*	0.921	0.960

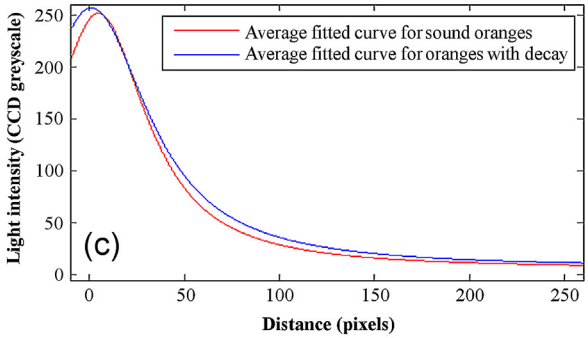

	Sound	Decaying
a (greyscale)*	6.22	7.60
b (greyscale)*	245.53	249.10
c (pixels)*	4.90	1.26
d (pixels)*	30.75	36.14
e (unitless)	0.998	0. 993

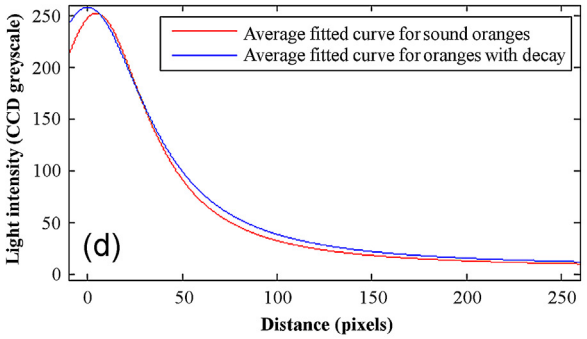

	Sound	Decaying
a (greyscale)*	6.83	7.38
b (greyscale)*	245.23	250.57
c (pixels)*	4.73	0.29
d (pixels)*	33.09	38.08
e (unitless)	0. 998	0. 999

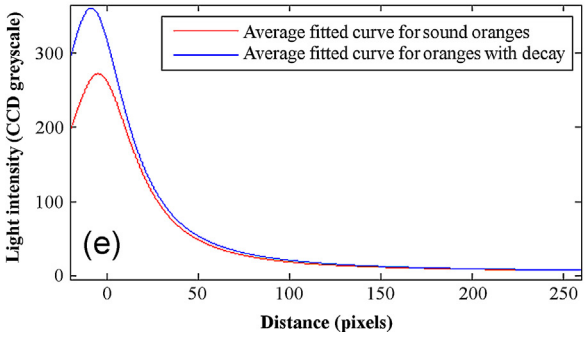

	Sound	Decaying
a (greyscale)	5.23	5.14
b (greyscale)*	266.93	355.48
c (pixels)*	-4.50	-8.40
d (pixels)*	24.16	23.42
e (unitless)	1.000	0.99

Fig. 5. Average Gaussian–Lorentzian cross product (GL) parameters and average GL distribution curves for the backscattering profiles of sound oranges and oranges with decay at: (a) 532 nm, (b) 660 nm, (c) 785 nm, (d) 830 nm, and (e) 1060 nm. Parameters marked with * presented statistically significant differences between sound and decaying oranges.

Table 2
Average determination coefficients (R^2) and average root mean squared errors (RMSE) from fitting backscattering profiles by the GL function for all samples at the five laser wavelengths.

Wavelength (nm)	R^2 (unitless)	RMSE (CCD greyscale)
532	0.998	2.14
660	0.999	0.61
785	0.998	2.48
830	0.998	2.54
1060	0.998	2.32

oranges were statistically significant. Some GL parameters presented a general trend at all the laser wavelengths (parameters *b*, *c* and *e*). The sound oranges had lower peak values (parameter *b*) than the oranges with decay at all wavelengths. By contrast, an opposite trend for centre values (parameter *c*) was observed, these being consistently higher for the sound oranges. However, the differences between both kinds of fruit for these two parameters were not significant enough at 660 nm. Furthermore, for both backscattering profiles, shape parameter (parameter *e*) generally had an almost constant value close to 1, even though this was slightly higher for the oranges with decay at 660 nm.

On the other hand, the asymptotic values (parameter *a*) and scattering widths (parameter *d*) showed a different trend between both backscattering profiles according to the laser wavelength. The sound oranges presented lower asymptotic values than the decaying oranges at almost every wavelength, except at 532 nm (parameter *a* was higher for the sound oranges) and at 1060 nm (parameter *a* did not present significant differences between both kinds of oranges). With regard to scattering widths, for the sound oranges, these values were lower than for the decaying oranges at 532, 785 and 830 nm and, conversely, higher at 660 and 1060 nm. From these results, it can be said that backscattering profiles, and consequently GL parameters, were dependent on the orange state: sound or decaying, since GL parameters differed between both states at the five laser wavelengths.

3.2. Classifier performance evaluation

Table 3 shows the classification results for the ranked wavelength combinations, obtained from the validation set of labelled data. Values of classification average success rate and Cohen's kappa statistic, as well as the corresponding confusion matrixes, are shown for all wavelength combinations. According to the scale proposed by Landis and Kock (1977), Cohen's kappa values were interpreted as follows: 0.00–0.20 regarded as slight, 0.21–0.40 as fair, 0.41–0.60 as moderate, 0.61–0.80 as good and 0.81–1.00 as very good.

When comparing the classification results, it can be noticed that the minimum average success rate of 80.39% and the lowest Cohen's kappa value of 0.610 were obtained for the single wavelength. In contrast, the best classification results were achieved using the five laser wavelengths with an average success rate of 96.08% and a value of Cohen's kappa of 0.921. As shown in the confusion matrix for this classification model using all the wavelengths, the percentage of well-classified fruit samples exceeded 95% for both classes despite the evident similarity between sound oranges and oranges with decay.

Moreover, the increase in the average success rate of around 10% from the single wavelength (80.39%) to the two-wavelength combination (90.20%) should be highlighted. Both wavelengths are in the visible wavelength range. Therefore, we assume that the visible wavelength range may provide more robust information on the differences in the scattering properties of the tissue, due to (i) higher scattering coefficients and resulting increased signal to noise ratio and (ii) increased perturbation in the NIR range due to highly variable water and carbohydrates contents that absorb in the NIR. From the corresponding confusion matrixes, it can be also observed that, while the number of well-classified sound oranges remained the same (87.50%) for both cases, the classification of oranges with decay was greatly improved for the two-wavelength combination, increasing from 74.07% to 92.59%. In practice, this reduction of the number of badly classified oranges with decay is of major importance for a potential inspection system since only a reduced number of infected and sporulated fruit can be the source for important spread of fungal infections to healthy fruit handled or stored in the packinghouse, thus causing great economic losses.

On the other hand, for all the other cases, from one wavelength combination to another, the increase in the average success rate was only approximately 2% by including one wavelength more in the model.

Effective control of green mould and other citrus postharvest diseases has relied for many years on the application of conventional synthetic chemical fungicides such as imazalil or thiabendazole. However, there is currently a clear need to find and implement alternative control methods because of increasing concerns about environmental contamination and human health risks associated with fungicide residues (Palou et al., 2008). Findings from this research are a significant step for the adoption by the citrus industry of nonpolluting alternative control methods, because early decay detection is an effective tool to reduce

Table 3
Classification results for the ranked wavelength combinations.

Number of wavelengths	Wavelength combination (nm)	Average success rate (%)	Cohen's kappa	Confusion matrix	
1	532	80.39	0.610	Sound (%)	Decay (%)
				Sound 87.50	25.93
				Decay 12.50	74.07
2	532, 660	90.20	0.803	Sound (%)	Decay (%)
				Sound 87.50	7.41
				Decay 12.50	92.59
3	532, 660, 1060	92.16	0.843	Sound (%)	Decay (%)
				Sound 91.67	7.41
				Decay 8.33	92.59
4	532, 660, 1060, 830	94.12	0.882	Sound (%)	Decay (%)
				Sound 95.83	7.41
				Decay 4.17	92.59
5	532, 660, 1060, 830, 785	96.08	0.921	Sound (%)	Decay (%)
				Sound 95.83	3.70
				Decay 4.17	96.30

fungicide usage in the context of integrated disease management (IDM) programmes.

4. Conclusions

The feasibility of laser-light backscattering imaging was proved for detecting superficial decay in citrus fruit caused by *P. digitatum*. Backscattering images of oranges at five laser wavelengths in the visible and NIR range were used for non-destructive detection. The GL distribution function with five independent parameters described backscattering profiles accurately, with average R^2 values higher or equal to 0.998. GL parameters were dependent on the orange state (sound or decaying), observing differences between both states at all wavelengths.

In the classification of sound and decaying oranges, all wavelengths contributed to the highest average success rate of 96.1%. The increase in the average success rate of around 10% from the single wavelength (80.4%) to the two-wavelength combination (90.2%), both in the visible range, should be highlighted.

Therefore, the early detection of decaying fruit by means of backscattering imaging analysis has a high potential for its integration in a commercial system. Nevertheless, for future setting up on a sorting line, perhaps a line laser should be applied on rotating fruit, instead of point lasers.

Acknowledgements

This work has been partially funded by the Instituto Nacional de Investigación y Tecnología Agraria y Alimentaria de España (INIA) through research project RTA2012-00062-C04-01 with the support of European FEDER funds. Delia Lorente thanks INIA for the support trough grant FPI-INIA number 42.

References

Barmore, C.R., Brown, G.E., 1981. Polygalacturonase from citrus fruit infected with *Penicillium italicum*. Phytopathology 71, 328–331.
Barmore, C.R., Brown, G.E., 1979. Role of pectolytic enzymes and galacturonic acid in citrus fruit decay caused by *Penicillium digitatum*. Phytopathology 69, 675–678.
Birth, G.S., 1976. How light interacts with foods. In: Gafney J.Jr. (Ed.), Quality Detection in Foods. ASAE, St. Joseph, USA, pp. 6–11.
Blasco, J., Aleixos, N., Gómez-Sanchis, J., Moltó, E., 2009. Recognition and classification of external skin damage in citrus fruits using multispectral data and morphological features. Biosystems Engineering 103, 137–145.
Cubero, S., Aleixos, N., Moltó, E., Gómez-Sanchis, J., Blasco, J., 2011. Advances in machine vision applications for automatic inspection and quality evaluation of fruits and vegetables. Food and Bioprocess Technology 4, 487–504.
Duda, R.O., Hart, P.E., Stork, D.G., 2001. Pattern Classification, second ed. Wiley-Interscience, New York.
Fisher, R., 1936. The use of multiple measurements in taxonomic problems. Annals of Eugenics 7, 179–188.
Fleiss, J.L., 1981. Statistical methods for rates and proportions, second ed. Wiley-Interscience, New York.
Gelman, A., Hill, J., 2006. Data Analysis Using Regression and Multilevel/Hierarchical Models. Cambridge University Press, New York.
Gómez-Sanchis, J., Martín-Guerrero, J.D., Soria-Olivas, E., Martínez-Sober, M., Magdalena-Benedito, R., Blasco, J., 2012. Detecting rottenness caused by *Penicillium* in citrus fruits using machine learning techniques. Expert Systems with Applications 39, 780–785.
Gómez-Sanchis, J., Blasco, J., Soria-Olivas, E., Lorente, D., Escandell-Montero, P., Martínez-Martínez, J.M., Martínez-Sober, M., Aleixos, N., 2013. Hyperspectral LCTF-based system for classification of decay in mandarins caused by *Penicillium digitatum* and *Penicillium italicum* using the most relevant bands and non-linears classifiers. Postharvest Biology and Technology 82, 76–86.
Kim, D.G., Burks, T.F., Qin, J., Bulanon, D.M., 2009. Classification of grapefruit peel diseases using color texture feature analysis. International Journal of Agricultural and Biological Engineering 2, 41–50.
Kurita, M., Kondo, N., Shimizu, H., Ling, P., Falzea, P.D., Shiigi, T., Ninomiya, K., Nishizu, T., Yamamoto, K., 2009. A double image acquisition system with visible and UV LEDs for citrus fruit. Journal of Robotics and Mechatronics 21, 533–540.
Landis, J.R., Kock, G.G., 1977. The measurement of observer agreement for categorical data. Biometrics 33, 159–174.
Limandri, S.P., Bonetto, R.D., Di Rocco, H.O., Trincavelli, J.C., 2008. Fast and accurate expression for the Voigt function. Application to the determination of uranium M linewidths. Spectrochimica Acta Part B 63, 962–967.
Lopes, L.B., VanDeWall, H., Li, H.T., Venugopal, V., Li, H.K., Naydin, S., Hosmer, J., Levendusky, M., Zheng, H., Bentley, M.V., Levin, R., Hass, M.A., 2010. Topical delivery of lycopene using microemulsions: enhanced skin penetration and tissue antioxidant activity. Journal of Pharmaceutical Sciences 99, 1346–1357.
Lorente, D., Blasco, J., Serrano, A.J., Soria-Olivas, E., Aleixos, N., Gómez-Sanchis, J., 2012a. Comparison of ROC feature selection method for the detection of decay in citrus fruit using hyperspectral images. Food and Bioprocess Technology, http://dx.doi.org/10.1007/s11947-012-0951-1.
Lorente, D., Aleixos, N., Gómez-Sanchis, J., Cubero, S., García-Navarrete, O.L., Blasco, J., 2012b. Recent advances and applications of hyperspectral imaging for fruit and vegetable quality assessment. Food and Bioprocess Technology 5, 1121–1142.
Lorente, D., Aleixos, N., Gómez-Sanchis, J., Cubero, S., Blasco, J., 2013. Selection of optimal wavelength features for decay detection in citrus fruit using the ROC curve and neural networks. Food and Bioprocess Technology 6, 530–541.
Lu, R., 2004. Multispectral imaging for predicting firmness and soluble solids content of apple fruit. Postharvest Biology and Technology 31, 147–157.
Lu, R., Cen, H., Huang, M., Ariana, D.P., 2010. Spectral absorption and scattering properties of normal and bruised apple tissue. Transactions of the ASABE 53, 263–269.
Martínez, A.M., Kak, A.C., 2004. PCA versus LDA. IEEE Transactions on Pattern Analysis and Machine Intelligence 23, 228–233.
Meinke, M., Friebel, M., 2009. Determination of optical properties of turbid media: continuous wave approach. In: Zude, M. (Ed.), Optical Monitoring of Fresh and Processed Agricultural Crops. CRC Press, Boca Raton, USA, pp. 44–55.
Mollazade, K., Omid, M., Tab, F.A., Mohtasebi, S.S., 2012. Principles and applications of light backscattering imaging in quality evaluation of agro-food products: a review. Food and Bioprocess Technology 5, 1465–1485.
Navarro, L., Pina, J.A., Juarez, J., Ballester-Olmos, J.F., Arregui, J.M., Ortega, C., Navarro, A., Duran-Vila, N., Guerri, J., Moreno, P., Cambra, M., Zaragoza, S., 2002. The citrus variety improvement program in Spain in the period 1975–2001. In: Proceedings of the 15th Conference of the International Organization of Citrus Virologists, IOCV, Riverside, pp. 306–316.
Palou, L., Smilanick, J., Usall, J., Viñas, I., 2001. Control postharvest blue and green molds of oranges by hot water, sodium carbonate, and sodium bicarbonate. Plant Disease 85, 371–376.
Palou, L., Smilanick, J.L., Droby, S., 2008. Alternatives to conventional fungicides for the control of citrus postharvest green and blue molds. Stewart Postharvest Review 2, 1–16.
Palou, L., Smilanick, J.L., Montesinos-Herrero, C., Valencia-Chamorro, S., Pérez-Gago, M.B., 2011. Novel approaches for postharvest preservation of fresh citrus fruits. In: Slaker, D.A. (Ed.), Citrus Fruits: Properties, Consumption and Nutrition. Nova Science Publishers, Inc., NY, USA, pp. 1–45.
Penache, C., Miclea, M., Bräuning-Demian, A., Hohn, O., Schössler, S., Jahnke, T., Niemax, K., Schmidt-Böcking, H., 2002. Characterization of a high-pressure microdischarge using diode laser atomic absorption spectroscopy. Plasma Sources Science and Technology 11, 476–483.
Peng, Y., Lu, R., 2005. Modeling multispectral scattering profiles for prediction of apple fruit firmness. Transactions of the ASAE 48, 235–242.
Qing, Z., Ji, B., Zude, M., 2007. Predicting soluble solid content and firmness in apple fruit by means of laser light backscattering image analysis. Journal of Food Engineering 82, 58–67.
Romano, G., Baranyai, L., Gottschalk, K., Zude, M., 2008. An approach for monitoring the moisture content changes of drying banana slices with laser light backscattering imaging. Food and Bioprocess Technology 1, 410–414.
Sierra, A., 2002. High-order Fisher's discriminant analysis. Pattern Recognition 35, 1291–1302.
Slaughter, D.C., Obenland, D.M., Thompson, J.F., Arpaia, M.L., Margosan, D.A., 2008. Non-destructive freeze damage detection in oranges using machine vision and ultraviolet fluorescence. Postharvest Biology and Technology 48, 341–346.
Stace, T.M., Truong, G.W., Anstie, J., May, E.F., Luiten, A.N., 2012. Power dependent lineshape corrections for quantitative spectroscopy. Physical Review A: Atomic, Molecular and Optical Physics 86, 012506-1–012506-5.
Wang, S., Li, D., Song, X., Wei, Y., Li, H., 2011. A feature selection method based on improved Fisher's discriminant ratio for text sentiment classification. Expert Systems with Applications 38, 8696–8702.
Weeks, A.R., 1996. Fundamentals of Electronic Image Processing. Wiley-IEEE Press.
Zude, M. (Ed.), 2009. Optical monitoring of fresh and processed agricultural crops. CRC, Press, Boca Raton, USA.